NUMERICAL ANALYSIS OF WAVE AND NEARSHORE CURRENT FIELDS AROUND LOW-CRESTED PERMEABLE DETACHED BREAKWATERS

Takeshi Nishihata[1], Yoshimitsu Tajima[2] and Shinji Sato[2]

A Boussinesq type numerical model was developed which can simulate both wave fields and current fields around permeable detached breakwaters. The validity of the model was verified through measurements of waves and nearshore currents in hydraulic experiments investigating reflection and transmission capability. The porosity of the structure was accounted by a friction term incorporating turbulent resistance. The combination of turbulent friction model and anisotropic diffusion type wave breaking model was found to reproduce wave fields around the detached breakwaters and nearshore current fields behind the structures with a good accuracy.

Keywords: permeable breakwater; porous structure; numerical modeling

INTRODUCTION

Recently, new-type permeable detached breakwaters, as shown in Figure 1, have been introduced along several coasts of Japan. These structures provide functions of both wave dissipation and littoral drift control. The former wave-dissipation function of the structure should be evaluated in terms of specific reflection coefficient in front of the structures and transmission coefficient behind the structures. Since low crest configuration is generally adopted to conserve coastal landscapes, overflow or wave breaking often happen on the top of the breakwaters. Consequently, complicated wave fields coupled with reflection, transmission, diffraction and breaking are observed in the vicinity of the permeable detached breakwaters. Understanding of such hydraulic condition and establishment for the estimation method are significant to design the tranquility and littoral drift control behind the structures.

For permeable detached breakwaters, many numerical analyses have been introduced, for example, by Izumiya (1990), Mizutani et al. (1995), Tajima(2005) for the wave fields and by Somchai et al. (1990) , Cruz et al. (1992) additionally for wave breaking. Furthermore, a few researches for the accompanied nearshore current have been done by Tajima et al. (2006) and Ranasinghe et al. (2009a). While above mentioned structures are conventional detached breakwaters which simply consist of a number of uniform materials such as rubble stones or wave dissipating concrete blocks, a new-type permeable detached breakwater (hereafter, we call it simply "*structure*") consists of wave-dissipating cells with precast concrete slit walls. Although several experimental studies and field observations have been executed for such structures especially focusing on the evaluations of the reflection and dissipation coefficients, no further studies have been done for wave and current field around the structure, the crest of which repeatedly emerges and submerges with wave breaking.

This paper aims to construct a numerical model for wave fields and nearshore current fields around the structures. We introduce the turbulent friction model inside the structure composed of various member materials to the non-linear dispersive wave theory and improve the wave breaking model to reproduce both wave fields and the nearshore current fields. The validity of the model is investigated through comparison with experimental data such as wave forms, dissipation capabilities and nearshore current fields.

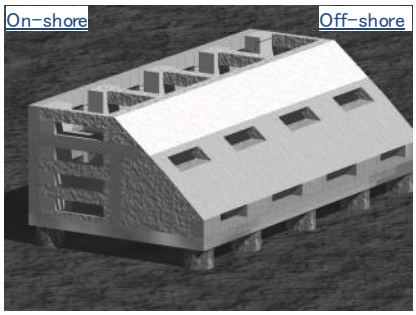

Figure-1. Example of new-type structure(S-VHS structure)

[1] Institute of Technology, Penta-Ocean Construction Co. Ltd., Yonku-cho 1534-1, Nasu-shiobara, Tochigi, 329-2746, Japan
[2] Departure of Civil Engineering, The University of Tokyo, Hongo 7-3-1, Bunkyo-ku, Tokyo, 113-8656, Japan

MODEL DESCRIPTIONS

This study applied the non-linear dispersive wave equations based on Madsen et al. (1997) modified Boussinesq model. The model is applicable to the calculation of porous media with arbitrary void ratios by which we model the permeable detached breakwaters or topography in the swash zone.

The continuity and momentum equations in our study are described as follows,

$$\alpha \frac{\partial \eta}{\partial t} + \frac{\partial P_i}{\partial x_i} = 0 \qquad (1)$$

$$\frac{\partial P_i}{\partial t} + \frac{\partial P}{\partial x_j}\left(\frac{P_i P_j}{A}\right) + gA\frac{\partial \eta}{\partial x_i} + \Psi_i + D_{f,i} + D_{b,i} = 0 \qquad (2)$$

where, η : water surface elevation, P : flow rate, α : void ratio at $z = \eta$, $A = h + \eta - (1-\varepsilon)z_l$: net depth, h : still water depth, ε : void ratio, z_l : thickness of porous media, g : gravity acceleration, Ψ : dispersion term, D_f : friction term, D_b : wave breaking term. Here, subscripts in the variables mean coordinate in the x_i axis ($i = 1,2$) where the summation rules are applied to the different subscripts. The variables used in the numerical analysis are summarized in the Figure-2.

For the analysis around the structure, some modifications are introduced and tried such as stabilization of advection term, turbulent friction and inspection of plural wave breaking models whose detailed expressions of the formulae are described in the following sections.

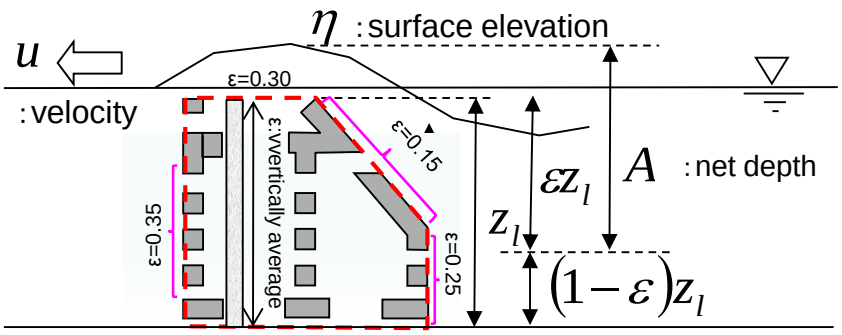

Figure-2. Variables used in the numerical analysis

Stabilization of the advection term

If u_i is the current velocity in the x_i direction, the advection term of the second term in the left-hand side of the equation (2) can be deformed as the following formula and be solved by a difference scheme.

$$\frac{\partial}{\partial x_i}\left(\frac{P_i^2}{A}\right) = u_i \frac{\partial P_i}{\partial x_i} + P_i \frac{\partial u_i}{\partial x_i} \qquad (3)$$

Spatial difference of the current velocity in the second term of the right-hand side often yields numerical instability in the vicinity of the abrupt depth change due to the structure. Ranasinghe et al. (2009b), who analyzed the wave overtopping on the submerged breakwaters using Nwogu(1993) type Boussinesq equations, succeeded to stabilize the computation when the crown of the submerged breakwaters dries up by introducing the sudden enlarged loss term to the advection term. We derived the deformed advection term implicitly including the same momentum loss in the Madsen type Boussinesq equation used in this study. First, assume the case if the current velocity u_i decreases to $u_i - \Delta u_i$ around the cross-section of sudden expansion as the Figure-3. The continuity equation at the position is described as,

$$A_{I-1/2} \cdot (u_i + \Delta u_i / 2) = A_{I+1/2} \cdot (u_i - \Delta u_i / 2) \qquad (4)$$

From which we could derive the following equation (5).

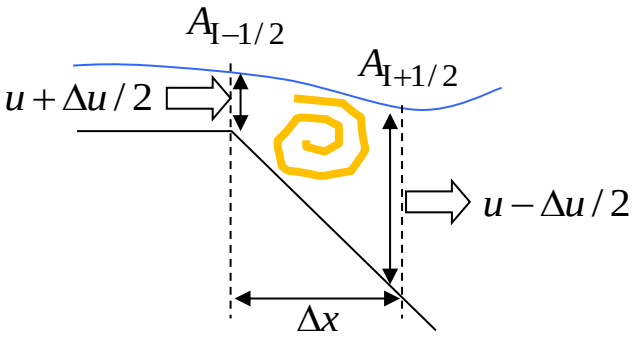

Figure-3. Sketch of sudden expansion and setting of variables

$$\frac{\partial u_i}{\partial x_i} = \left(A_{I,x} / A_I\right) u_i \qquad (5)$$

Besides, vertically averaged energy loss ratio is denoted as the following equation (6).

$$1/\Delta t \int_{bottom}^{surface} \left[\frac{(u_i + \Delta u_i / 2)^2}{2} - \frac{(u_i - \Delta u_i / 2)^2}{2} \right] dz = A_I \frac{\partial}{\partial t} \frac{1}{2} {u_i}^2 \qquad (6)$$

Equivalent momentum loss ratio to the equation (6) can be expressed by using the equation (5),

$$\begin{aligned} R_N &= A_I \Delta u_i / \Delta t \\ &= A_I \Delta u_i / \Delta x_i \cdot \Delta x_i / \Delta t \qquad (7) \\ &= A_I \frac{\partial u_i}{\partial x_i} = {u_i}^2 A_{I,x} \end{aligned}$$

Now, adding it to the advection term (3) leads to the following transformed advection term,

$$\begin{aligned} \frac{\partial}{\partial x_i}\left(\frac{{P_i}^2}{A_I}\right) + R_N &= u_i P_{i,x} + P_i u_{i,x} + u^2 A_{I,x} \\ &= u_i P_{i,x} + u_i \left(A_I u_{i,x} + u_i A_{I,x}\right) \qquad (8) \\ &= 2u_i \frac{\partial P_i}{\partial x} \end{aligned}$$

Equation (8) is numerically stable because it only contains the derivative term of flow rate. The advection term (3) should be exchanged by the equation (8) in the vicinity of the structure's boundary where the net depth significantly changes if the direction of flow coincides with that of the turbulence generation.

Friction Term

In the equation (2), D_f represents resistance term generally expressed by the law of Dupuit-Forchheimer which consists of laminar, turbulent and inertia resistance terms. However, the coefficients incorporated with each resistance term could be determined through some hydraulic experiments (for instance, van Gent(1995)), submission of a general formula for new type permeable structures is difficult because many kinds of shapes and materials of them has been proposed and porosity differs heterogeneously from each member of frameworks. Here, we define the resistance effect from the structure as to be proportional to the square of the current velocity, that is, only considering the turbulent resistance effect like equation (9). Energy dissipation is accounted from not only the friction but the wave breaking effect explained in the next chapter because wave breaking is frequently induced on the low-crested structures,

$$D_{f,i} = -f \frac{z_l \varepsilon}{A} u_i |u_i| \qquad (9)$$

where f is identical to the friction coefficient whose value is described later.

Wave Breaking Term

For the diffusion coefficient accompanied by wave breaking, the following model which is applicable to submerged block dikes with level crests (Tajima et al., 2006) is used.

$$\nu_T = f_D \frac{gd}{\omega^2} = \begin{cases} 2.5 \tan\beta \dfrac{\gamma_s^2}{\gamma^2} \dfrac{\gamma^2 - \gamma_r^2}{\gamma_s^2 - \gamma_r^2} \sqrt{\dfrac{g}{d}} \dfrac{gd}{\omega^2} & (\beta \neq 0) \\ 0.094 \left(1 - \dfrac{\gamma_r^2}{\gamma^2}\right) \sqrt{\dfrac{g}{d}} \dfrac{gd}{\omega^2} & (\beta = 0) \end{cases} \quad (10)$$

$$\gamma_s = 0.3 + 4\tan\beta \quad (11)$$

Here, ν_T : diffusion coefficient, d : mean net depth, ω :angular frequency, β : bottom slope, γ : ratio of current velocity to wave celerity, γ_s : ratio of the breaking wave height to breaking depth when it asymptotically becomes constant, γ_r : ratio of the breaking wave height to breaking depth when breaking wave is reborn. Wave breaker index is decided from the ratio of current velocity to wave celerity which we supposed γ more than 0.8 as to be consistent with the experimental results in the next chapter. Diffusion coefficient, as introduced by Hirayama and Hiraishi (2004), is given by solving the advection, diffusion, generation and dissipation of the turbulent energy so that it is spatially smoothed as below,

$$\frac{\partial k}{\partial t} + \frac{P_i}{A}\frac{\partial k}{\partial x_i} - \frac{\partial}{\partial x_j}\left(\nu_T \frac{\partial k}{\partial x_j}\right) = P_* - \frac{C_D k^{3/2}}{l_t} \quad (12)$$

$$\nu_T = \sqrt{k} l_t \quad (13)$$

$$P_* = \frac{C_D}{l_t}\left(\frac{\nu_T}{l_t}\right)^3 \quad (14)$$

P_* represents turbulence generation term in steady-state condition, $l_t = 1.5H_0$, $C_D \approx 0.09$, H_0 means offshore wave height.

We have studied sponge type and anisotropic diffusion type wave breaking model, the former of which cause the similar energy dissipation effect as laminar resistance. The validity will be inspected through the experiments in the next chapter. Watanabe and Dibajnia (1988) model is used for the sponge type wave breaking model in our study as below,

$$D_{b,i} = f_D P_i \quad (15)$$

f_D can be determined by the inversion calculation of equation (10).

For the diffusion type wave breaking model, anisotropic diffusion type wave breaking model as following equations introduced by Tajima et al. (2006) is used. In the anisotropic diffusion model, the diffusion coefficient defined by the equation (10) is applied to the primary direction of the wave only, which aims to improve the computational accuracy around the submerged breakers with apertures.

$$D_{b,i} = -\frac{\partial}{\partial x_j}\left(\nu_{ij} \frac{\partial P_i}{\partial x_j}\right) \quad (16)$$

$$\begin{pmatrix} \nu_{11} & \nu_{12} \\ \nu_{21} & \nu_{22} \end{pmatrix} = \begin{pmatrix} \nu_T \cos^2\theta & \nu_{LK} \\ \nu_{LK} & \nu_T \sin^2\theta \end{pmatrix} \quad (17)$$

$$\nu_{LK} = \Lambda U_w H \quad (18)$$

where, $\Lambda \approx 0.1$, U_w :particle velocity at the bottom, H :wave height, θ :wave direction when wave breaking(defined 0 for the on-shore direction).

HYDRAULIC MODEL EXPERIMENTS AND REPRODUCTIVE COMPUTING

Cross-sectional Wave Flume Experiments and Parameter Study

Numerical models for the low-crested permeable detached breakwaters has been verified with the cross-sectional wave flume experiments executed by Anno and Nishihata(2010). The Experimental condition has been decided to refer to the feasibility condition of the shore where actual permeable detached breakwaters had been constructed. We suppose monochromatic wave experiments with various wave periods and 1/25 model scale. Tabel-1 indicates experimental cases and Figure-4 shows the experimental setting.

Table 1. Experimental cases in the cross-sectional wave basin

case	Wave Height(cm)	Wave Period(s)
1	12.0	1.6
2	12.0	2.0
3	12.0	2.4
4	12.0	2.8

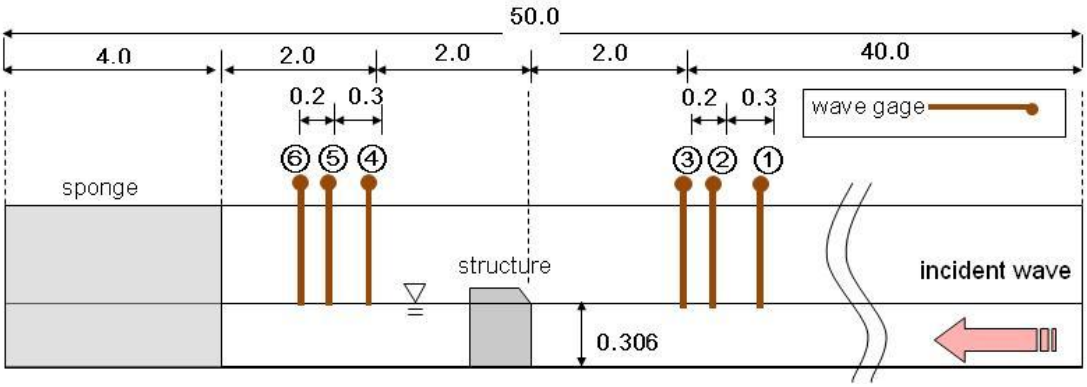

Figure 4. Setting of the cross-sectional wave flume experiment

In the numerical analyses, structures are modeled by using vertically averaged void ratio referring to the configuration of the members of the frameworks(see, figure-5). The spatial grid size is set to 2cm and the local porosity distribution is fitted to the actual structure. The void ratio of the overall structure in the numerical model becomes 0.60 which agrees with the actual structure's void ratio 0.61. The coefficient of the turbulent friction f is changed from 0.0 to 2.0 and is optimized by the sensitivity analyses. Reflection and transmission coefficients solved by Goda et al. (1976) separation method of the incident and reflection waves for each analysis and experiment are demonstrates in the Figure-6 and time series of the surface elevation of each friction coefficient is shown in the Figure-7. In this figures, sponge type wave breaking model is used in computation, besides little difference is seen in the analytic results by using the anisotropic diffusion type wave breaking model.

If the coefficient is assumed 1.0, wave height distribution in front and behind the structure, in other words, reflectance and transmittance is conformable and drifts of water surface elevation in the experiments and numerical analyses coincide with each other. When spatially uniform void ratio 0.6 is given, worse analytic results in the surface fluctuation have been gained so it is necessary to give the local variation of the void ratio accurately for the numerical model. Thus, we suppose the coefficient f to 1.0 in this study.

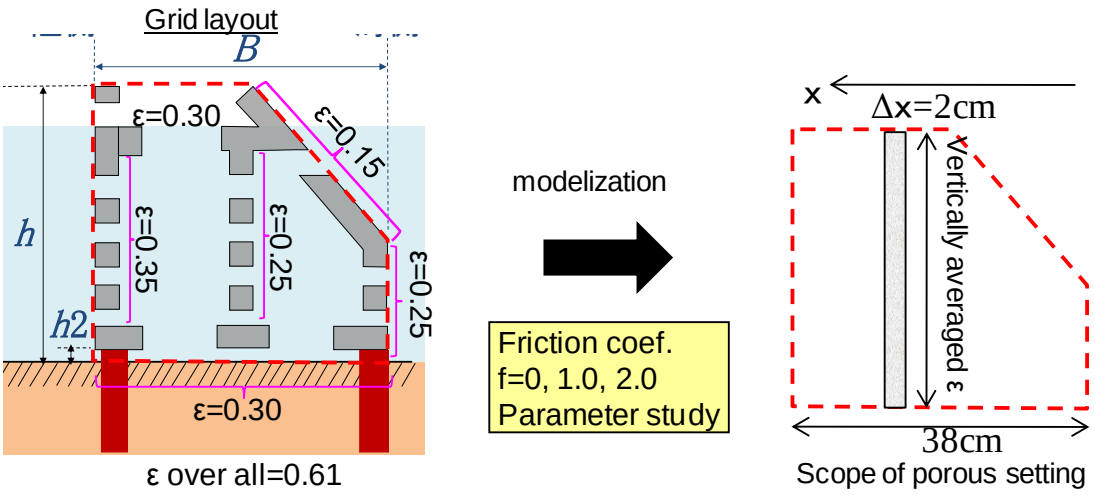

Figure 5. Given void ratio in the numerical analyses(left figure : member of framework with various void ratio, right : vertically averaged void ratio for computation)

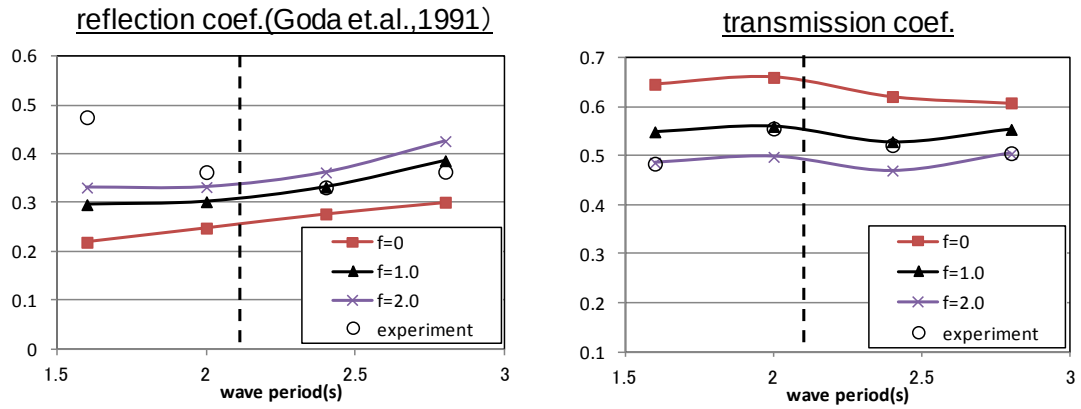

Figure 6. Comparison of wave dissipation ability between computation and experiments (left : reflectance, right : transmittance)

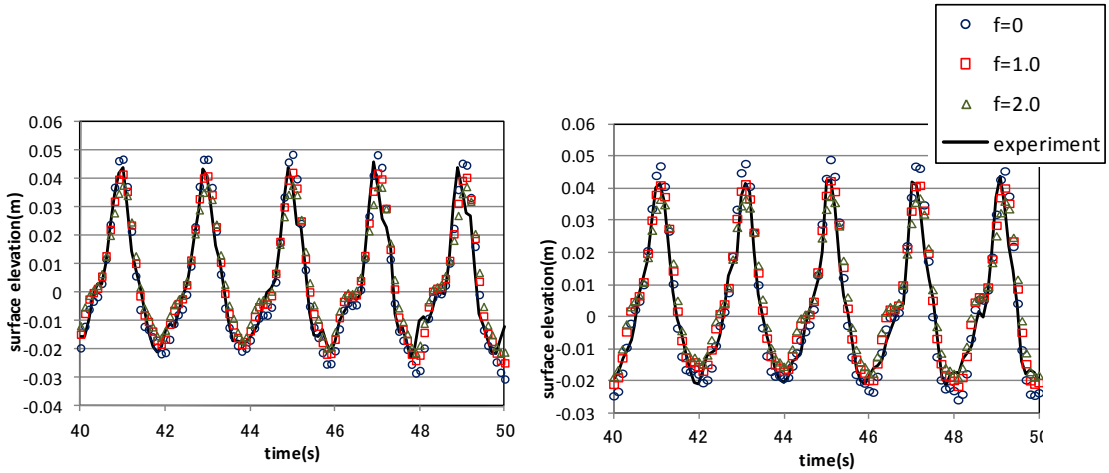

Figure 7. Examples of the water surface fluctuation with various friction coefficients

Large wave tank experiment for waves and current fields around the structures

In the large wave tank experiment, 2 types of the waves are generated and supposed as the usual and rough sea condition of one directional regular waves, 5cm and 12cm of wave height with 0 degree and 20 degree of wave direction. Experimental cases are summarized in Table-2, planer and cross-sectional view are shown in the Figure-8. In the experiments, wave generator boards are controlled to absorb the reflection waves. Perfect wave reflection condition is formed on the side boundaries to arrange the wave inducing wall. Hydraulic model of the structures consists of 5 cells as one set. 3 sets of hydraulic models are put into the wave basin as Figure-8. As control experiments, experiments with no structure are executed under the same condition of those with structures. Nevertheless model scale of the experiments is less than that in the cross-sectional experiments, almost similar configuration model is used. Wave period in the large wave tank experiments is 1.5s which is identical to 2.1s of the wave period in the cross-sectional wave experiments considering the model scale and similarity law, in which both wave reflection and transmission ability is expected to be reappeared well in the numerical simulation. Capacitance-type wave gages and electromagnetic current meters are installed around the structures to grasp the wave fields and current fields in the neighbor of the structures. Wave gages are also settled on the measuring cargo, which are able to move in the cross-shore and long-shore direction and measure wave height and mean water surface elevation by 50cm interval during wave generation from the vicinity of the structures to the shoreline. Furthermore, current field analyses of the video images using PTV method(Shimozono et al., 2005) are carried out in the partial area around the aperture between the first and second set of the structure. Under the usual wave condition with no model, waves break at 0.5m off the shoreline, besides, under the rough sea condition, wave breaking point is seen at 1.5m off the shoreline. Visual inspection of the floats thrown into the breaker zone certifies the nearshore current accompanied by the wave breaking in the experiments with oblique incident waves (20 degree). When waves of rough sea condition are generated in the flume with structures, strong nearshore current toward off-shore direction also could be observed at the aperture between structures (Figure-8).

Table 2. Experimental cases in the large wave basin

Case	Structures (set)	Wave condition	Wave Height(cm)	Wave Period(s)	Wave Direction(deg)
1	0	Usual state	5	1.5	0
2	3				
3	0				20
4	3				
5	0	Rough sea	12		0
6	3				
7	0				20
8	3				

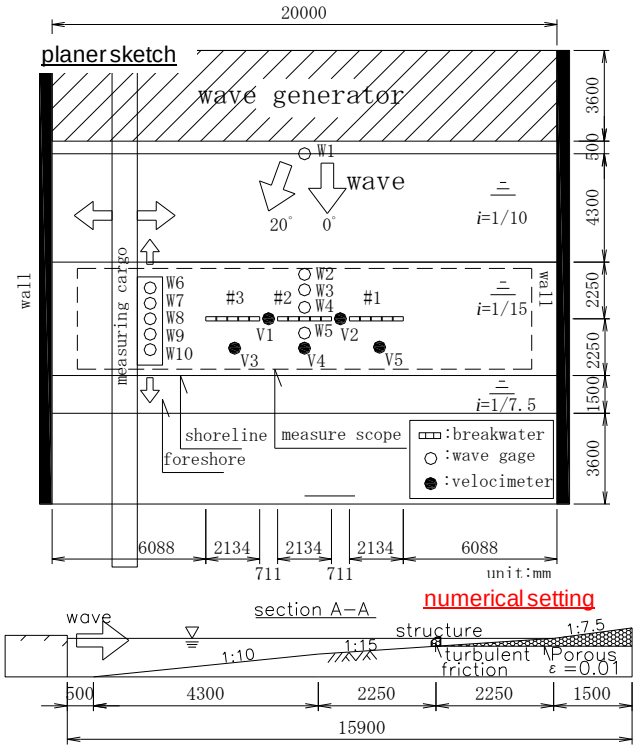

Figure 8. Planer sketch of the large wave tank experiment (upper) and cross-sectional view(lower)

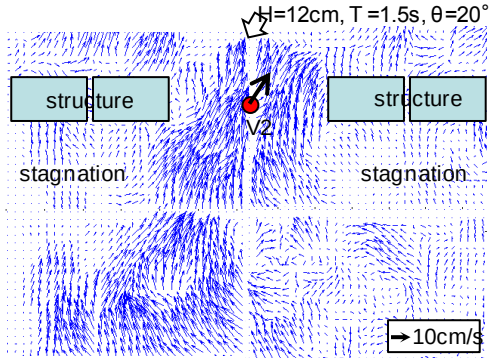

Figure 9. Current field obtained from PTV method(Case 8)

Numerical analyses to reproduce large wave tank experiments

Cross-sectional bathymetry and numerical setting demonstrated in the figure-8 is used in duplication analyses of the large tank experiments. Friction term expressed by equation (9) and porous layer are arranged in the simulation as well as the cross-sectional wave flume experiments. The bottom slope at the swash zone is modeled by the porous of low void ratio in order to improve the appearance of nearshore current inside the breaker zone. Numerical computation is conducted for each wave breaking model of the sponge type in equation (15) and diffusion type in equation (16). Examples of wave height, mean water surface elevation and current distribution in the observations and analyses under the usual wave conditon(case 4) and the rough sea condition(case 8) are demonstrated in Figures-10 to Figure-13. Here, mean water surface elevation and current velocity are defined as the average during two periods from the end of the simulation time.

Computing with sponge type wave breaking model presents accurate wave height distribution around the structures and can analyze the rip current at the aperture between structures which is seen on rough sea condition. However, nearshore current in the breaker zone accompanied by oblique incident waves cannot be analyzed. As Tajima et al. (2006) pointed out, the wave breaking model seems to smooth the nearshore current along the longshore direction excessively near the wave breaking point because it

gives the dissipation due to wave breaking as the resistance coefficient(laminar resistance) in proportion to the current velocity independent of the wave direction.

On the other hand, computing with diffusion type wave breaking model also provides accurate wave height distribution around the structure as well as the sponge type wave breaking model. Concerning with the nearshore current, it successfully analyzes not only rip current toward off-shore at the aperture of the structure and stagnation behind the structures on rough sea condition but also longshore current associated with the wave breaking of the oblique incident waves in no relation to wave height.

From above discussion, it turns out that the combination use of the method how to set friction coefficient and wave breaking models presented in this study could solve the wave fields around the low-crested detached breakwaters practically well. Nevertheless, anisotropic diffusion type wave breaking model to solve nearshore current more accurately is useful when considering the sediment transport around or behind the structures.

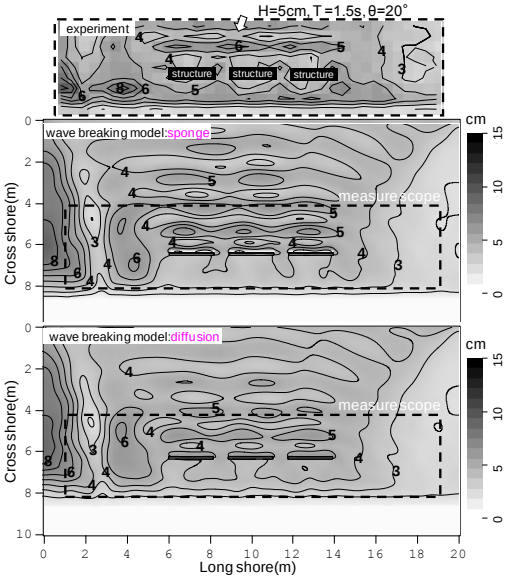

Figure 10. Wave height distribution(case4) (upper : experiment, middle : sponge type model, lower : diffusion type model)

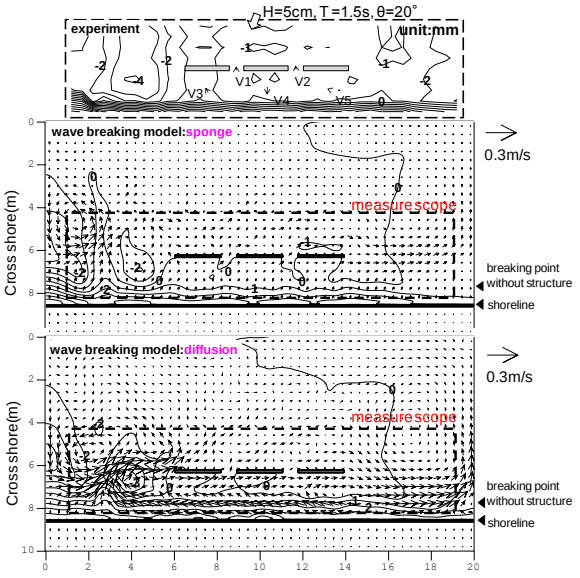

Figure 11. Mean water elevation and current field(case4) (upper : experiment, middle : sponge type model, lower : diffusion type model)

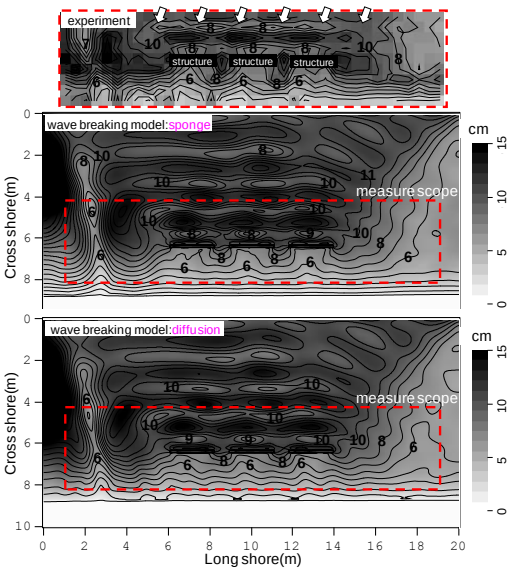

Figure 12. Wave height distribution(case8) (upper : experiment, middle : sponge type model, lower : diffusion type model)

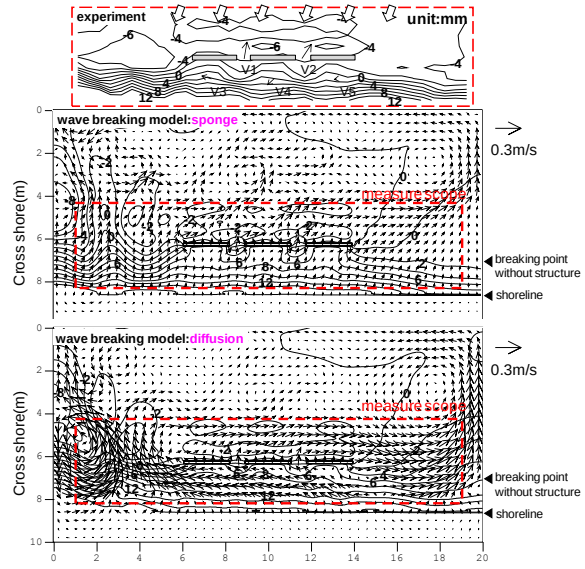

Figure 13. Mean water elevation and current field(case8) (upper : experiment, middle : sponge type model, lower : diffusion type model)

CONCLUSIONS

A numerical model based on non-linear dispersive wave theory with porous media to analyze the complex wave and current fields around a low-crested permeable detached breakwater was proposed and tested with experiments. Concluding remarks are summarized below.

(1) Both transmission and reflection can be appropriately computed when an optimum turbulent friction coefficient and vertically averaged void ratio consistent with structure configuration are given for a low-crested permeable detached breakwater.

(2) Anisotropic diffusion type wave breaking model improves the predictive skills of the nearshore current field around the structure significantly.

ACKNOWLEDGEMENTS

Experiments in this paper were carried out in the hydraulic facilities of the Penta-Ocean Construction Co. Ltd. We note here our appreciation for the cooperation of people involved in the experiment.

REFERENCES

Anno, K., and T. Nishihata. 2010. Development on offshore structure with wave force reduction, *Proceedings of 32th International Conference on Coastal Engineering*, ASCE, 224.

Cruz, E., K. Shiba, M. Isobe and A. Watanabe. 1992. A Computational Method for two-dimensional nonlinear wave transformation over submerged permeable breakwaters, *Proceedings of Coastal Engineering*, JSCE, Vol.39, 621-625.

Goda, Y., Y. Suzuki, Y. Kishira and O. Kikuchi. 1976. Estimation of incident and reflected waves in random wave experiments, *Technical Note of PARI*, No.248, 1-28.

Hirayama, K., and T. Hiraishi. 2004. Boussinesq modeling of wave breaking and run-up on a reef;1D, , *Proceedings of Coastal Engineering*, JSCE, Vol.51, 11-15.

Madsen, P. A, O. R. Sorensen and H. A. Schaffer. 1997. Surf zone dynamics simulated by a Boussinesq type model. Part 1. Model description and cross-shore motion of regular waves, *Coastal Engineering*, ASCE, 255-287.

Mizutani, N., T. Goto, and W. G. McDougal. 1995. Hybrid-type numerical analysis of wave transformation due to a submerged permeable structure and internal flow, *Proceedings of Coastal Engineering*, JSCE, Vol.42, 776-780.

Nwogu, O.J. 1993. Alternative form of Boussinesq equations for nearshore wave propagation, *Journal of waterways, Port, Coastal and Ocean Engineering*, ASCE, Vol.119(6), 618.

Ranasinghe, R. S, S. Sato and Y. Tajima. 2009a. Modeling of waves & currents around porous submerged breakwaters, *Coastal Dynamics*, No.12.

Ranasinghe, R. S, S. Sato and Y. Tajima. 2009b. Boussinesq modeling of waves and currents over submerged breakwaters, *APAC*, Vol.13, 58-64.

Rojanokamthorn, S., M. Isobe, and A. Watanabe. 2007. Modeling of wave transformation on submerged breakwater, *Proceedings of 22th International Conference on Coastal Engineering*, ASCE, 1060-1073.

Shimozono, T., S. Sato, and M. Isobe. 2005. Control of nearshore current and beach deformation by submerged detached breakwater, *Asian and Pacific Coast*, Vol.13, 1139-1153.

Tajima, Y., M. Kozuka, K. Ooshima and Y. Moriya. 2006. Numerical study on the effect of porous submerged mound to dissipate non-breaking long waves, *Proceedings of 30th International Conference on Coastal Engineering*, ASCE, 5008-5020.

Tajima, Y., S. Sato, T. Shimozono and M. Isobe. 2007. Modeling of wave-induced current around submerged detached breakwaters, *Proceedings of International Conference on Coastal Structures*, ASCE, 725-736.

Van Gent, M. R. A. 1995. Porous flow through rubble-mound material, *Journal of waterways, Port, Coastal and Ocean Engineering*, ASCE, 121(3), 171-181.

Watanabe, A. and M. Dibajnia. 1988. A numerical model of wave deformation in surf zone, *Coastal Engineering*, ASCE, 578-587.